# EFFECT OF THERMAL ANNEALING ON THE ELECTROCHEMICAL AND MAGNETIC PROPERTIES OF LITHIUM FERRITE NANOPARTICLES

[1*]P. Hajasharif, [1] K. Ramesh, [2] S. Sivakumar, [3] P. Sivagurunathan
[1*]Assistant Professor, [1]Research Scholar, [2]Assistant Professor, [3]Professor
[1*]Department of Physics, Arignar Anna Government Arts College, Villupuram, Tamilnadu, India.
[1,2,3] Department of Physics, Annamalai University, Annamalai Nagar, Tamilnadu, India.

***Abstract:*** The $Li_{0.5}Fe_{2.5}O_4$ nanoparticles were effectively synthesized using the sol-gel method. The synthesized materials were calcinated at the different temperatures (600 °C, 700 °C, and 800 °C) for 5 hours. The structural properties, morphology, magnetic impedance spectroscopy and electrochemical study of the $Li_{0.5}Fe_{2.5}O_4$ nanoparticles were identified with the help of characterization by using TG/DTA, XRD, FT-IR, FE-SEM with EDAX, VSM, and CV. The synthesized material was first characterized by using Thermo gravimetric analysis / Differential thermal analysis (TGA/DTA) from this study there are three major weight losses are noted. The X-ray diffractogram reveals in the formation of single phase with cubic structure. Mean crystallite size and lattice parameter also calculated using XRD data. FT-IR spectrum confirms that the vibration of tetrahedral and octahedral frequencies of prepared samples. The structural morphology analysis confirms by FE-SEM it was some agglomerated with similar spherical structure. The energy dispersive X-ray analysis technique is used for identifying the elemental composition of the sample. VSM study confirms the M-H loops of lithium ferrite nanoparticles and formation of ferromagnetic nature. The CV study confirms the $Li_{0.5}Fe_{2.5}O_4$ nanoparticles are pseudo capacitive nature and estimated specific capacitance is 569 $Fg^{-1}$ for the lowest scan rate at 10 $mVs^{-1}$.

***Keywords*:** Lithium Ferrite, XRD, FT-IR, FE-SEM with EDAX, VSM, and CV

## 1. Introduction

The inorganic materials are mostly used in conventional energy applications along with materials and material blends for the potential future energy systems [1]. The field of ferrites is very primitive, but significant one. Due to their various potential applications and interesting physics involved in it, even after more than half-a century scientist, researchers and engineers are still interested in a various types of ferrite materials prepared by the different techniques and its various properties as a function of compositions, temperature, frequency, etc., [2]. Lithium ferrite is commercially available ferrite used in different types of applications, such as: electromagnetic absorbers, fuel cells, sensors and microelectronic materials, due to its stability, low conductivity, stress sensitivity and high cure temperature [3]. $Li_{0.5}Fe_{2.5}O_4$ is an inverse spinel with a cubic structure, the $Li^+$ monovalent ions are occupying in B sites and $Fe^{3+}$ ions are occupying in A and B sites [4]. Disordered structure is the generally inverse spinel structure with space group Fd3m and ordered structure corresponds to space group P4332 [5]. Bulk lithium ferrite is the inverse spinel that typically crystallizes in two polymorphic forms [6,7]. $Li_{0.5}$ $Fe_{2.5}$ $O_4$ nanoparticles can be synthesized by various chemical methods, such as Flash combustion method, citrate precursor method, standard ceramic method, aerosol method, mechano chemically method, co-precipitation method, and hydrothermal method [8, 9, 10]. Among these methods, sol-gel method is better than other methods achieved a smaller grain size, homogeneity and better crystalline nature. In this paper, we attempt to synthesize of lithium ferrite nanoparticles using sol-gel method. Synthesized lithium ferrite nanoparticles characterized by the following techniques TG/DTA, XRD, FT-IR, FE-SEM with EDAX, VSM and CV.

## 2. Experimental procedure

### 2.1 Materials and Method

All these chemical reagents were purchased done from the Merck (grade AR) with 99% purity and used without any other further purification. For materials reagents such as Li $(NO_3)_2$ .$6H_2O$, Fe $(NO_3)_2$.$9H_2O$ by the lithium ferrite nanoparticles synthesized by sol-gel method. From the preparation of lithium ferrite nanoparticles are shown in fig. 1. The precursor material was done by different molar ratio 1:2 for Li $(NO_3)_2$*$6H_2O$, Fe $(NO_3)_2$ *$9H_2O$ and 50 ml of de-ionized water added separately and homogeneity dissolved in precursor and appropriate amount of ethylene glycol with dissolved in 50 ml of de-ionized water added separately, and continuously stirred at 650 rpm. Then, the dissolved solution was magnetically stirred for 6 hours at 70 °C. Finally a gel was formed, the collected gel was dried in the oven to form the $Li_{0.5}Fe_{2.5}O_4$ powder at 100 °C for 2 hrs and calcined at different temperatures of 600 °C, 700 °C, and 800 °C.

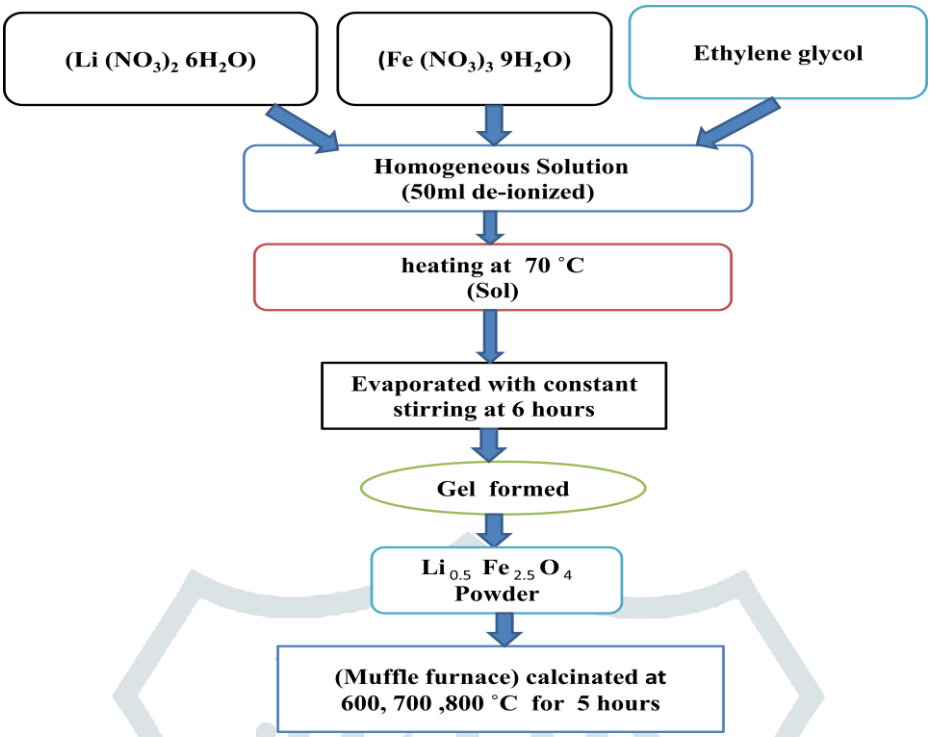


**Fig. 1 Flow chart for preparation of lithium ferrite nanoparticles**

The preparation of lithium ferrite nanoparticles depicts the TG/DT analysis of $Li_{0.5}Fe_{2.5}O_4$ nanoparticles. TG/DT analysis can be performed using the instrument Netzsch-Sta 449 F3 Jupiter with a heating rate of 10 °C $min^{-1}$ under air atmosphere. The phase formation of the $Li_{0.5}Fe_{2.5}O_4$ nanoparticles was characterized by X-ray diffraction (XRD) using PW3040/60 X'pert PRO powder X-ray diffractometer with CuKa radiation ($\lambda$ =1.5418Å) at 40 kV and 30 mA. The step scans were performed for 2h values in the angular series of 10 °C to 80 °C with a scanning speed of 10 $min^{-1}$. The Functional group of analyses was recorded 4000 to 400 $cm^{-1}$ on a Shimadzu FT-IR 8201PC infrared spectrometer. FE-SEM Analysis helps used for size of the morphology were performed using JEM 2100F. Magnetic measurements were carried out at room temperature using a lakeshore 7410 vibrating sample magnetometer (VSM) with a maximum magnetic field 20 kOe. An electrochemical measurement was performed by cyclic voltammeter (CV) model CHI 660.

## 3. Results and Discussions

### 3.1 TG/DT analysis

TGA and DTA study of as-prepared $Li_{0.5}Fe_{2.5}O_4$ nanoparticles were recorded in a stationary air atmosphere from 35 °C to 1100 °C. Fig.2 depicts the TG/DT analysis of $Li_{0.5}Fe_{2.5}O_4$ nanoparticles there are three major weight losses can be found in TGA curve.

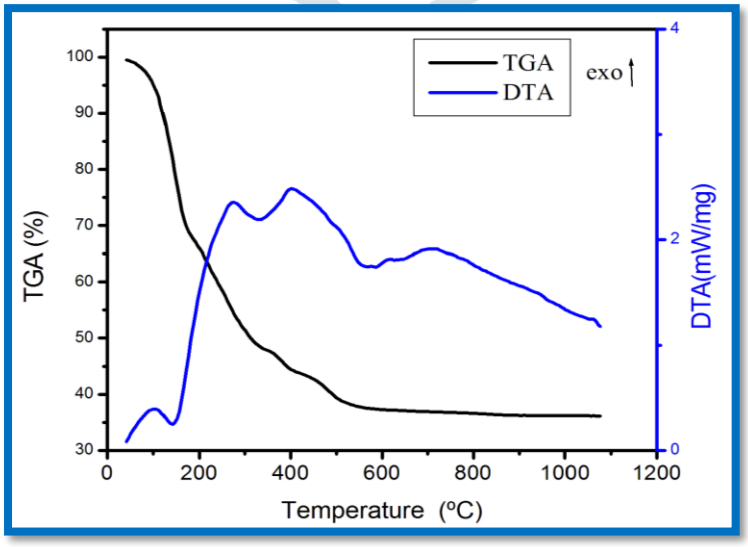


**Fig.2 TG/DT analysis of $Li_{0.5}Fe_{2.5}O_4$ nanoparticles**

The 1st weight loss observed at a temperature below 173 °C (31%) due to desorption of water. The 2nd weight loss observed in the range of 174 °C to 337 °C (21%) due to organic templates. 3rd weight loss is 338 °C to 556 °C (11%) attributed to the formation of crystallization turning point. No more weight loss predicted above 556 °C, representing the stable phase of $Li_{0.5}Fe_{2.5}O_4$ nanoparticles. From the DTA curve showed a minute endothermic peak at a 139 °C owing dehydration of water molecules. The exothermic points from 103 °C, 277 °C and 404 °C is attributed outstanding to the decomposition of nitrates and initiates of crystallization formation of $Li_{0.5}Fe_{2.5}O_4$ nanoparticles. Therefore, after dehydration, the anhydrous precursor passes through the decomposition to produce lithium ferrite. The endothermic point at 138, 330 °C and 563 °C corresponds to the absolute decomposition, but ethylene glycol to form the $Li_{0.5}Fe_{2.5}O_4$ with the simultaneous evolution of CO, $CO_2$ and acetone molecules created. Related behavior reported by Dey et al., [11] for $Li_{0.5}Fe_{2.5}O_4$ nanoparticles using the sol - gel method

## 3.2 XRD analysis

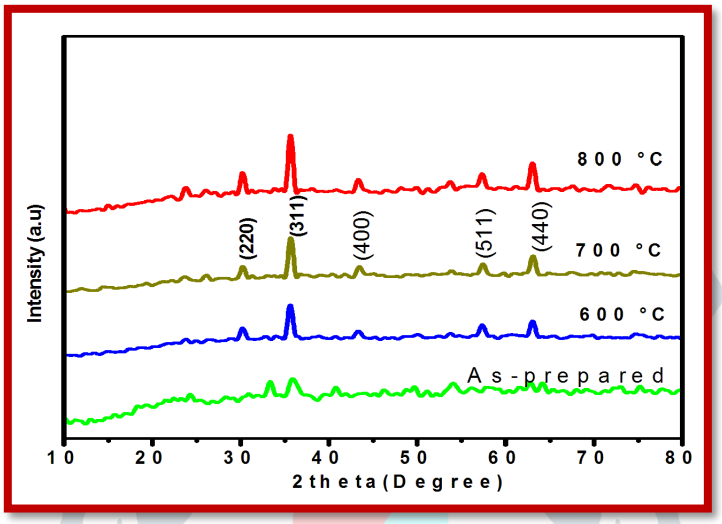


**Fig. 3 X-ray diffraction Pattern of $Li_{0.5}Fe_{2.5}O_4$ nanoparticles**

Fig.3 shows that the X-ray diffraction of $Li_{0.5}Fe_{2.5}O_4$ nanoparticles as-prepared, calcinated at 600 °C, 700 °C and 800 °C. As-prepared sample shows not clearly identified due to impurity phase detected in the sample, while the calcinations are major role of synthesized nanoparticles. The calcinated sample exhibits, but mutually reflections of h k l planes are (220), (311), (400), (511) and (440) [12]. The reflection peaks indicate in the present study clearly specify the structure of $Li_{0.5}Fe_{2.5}O_4$ nanoparticles without impurities. The reflected peaks perfectly well matched with the standard JCPDS card no. 49-0266 with a cubic spinel structure with the Fd3m group. The mean crystallite size was calculated from given the Debye Sherrer's formula $D = 0.9\lambda / \beta\cos\theta$ Here, λ is the wavelength of the Cu Ka radiation (λ =1.5418Å), ß is the full width half maximum. Lattice parameter 'a' can be calculated using the relation $a = d_{hkl} (h^2 + k^2 + l^2)^{1/2}$ Where, d is the inter planner distance and h, k, l are the miller index.

**Table 1 Structural parameter**

| Temperature (°C) | Crystallite size (nm) | Lattice Parameter (Å) |
|---|---|---|
| As-prepared | 16 | 8.929 |
| 600 | 36 | 8.303 |
| 700 | 38 | 8.321 |
| 800 | 49 | 8.334 |

From the Table1 shows that, As-prepared, 600 °C, 700 °C and 800 °C mean crystallite size was increased due to the growth of $Li_{0.5}Fe_{2.5}O_4$ nanoparticles. Calculated lattice parameter increased from 8.303 (Å), 8.321 (Å), 8.334 (Å) with the increases in the calcinations temperature from 600 °C, 700 °C, and 800 °C. In this study imply that the uniformly increasing the lattice parameter of the system with the calcinations temperature and also tabulated. The tendency obeys that vagard's law the replacement of ions $Li^{1+}$ ions (monovalent) at an octahedral (B) site and $Fe^{3+}$ ions is occupying in tetrahedral (A) sites and octahedral (B) sites.

## 3.3 FT-IR analysis

Fig.4. Shows that the FT-IR study of $Li_{0.5}Fe_{2.5}O_4$ nanoparticles was recorded in the range of 4000 to 400 $cm^{-1}$. The absorption band around at 600-400 $cm^{-1}$ corresponds to the presence of metal oxygen vibration of $Li_{0.5}Fe_{2.5}O_4$ nanoparticles. In the low frequency vibrations of ($\upsilon_2$) 475 $cm^{-1}$ is associated to the metal oxide stretching vibrations in the octahedral sites with

additional bands of about 1421 $cm^{-1}$ and 1570 $cm^{-1}$.

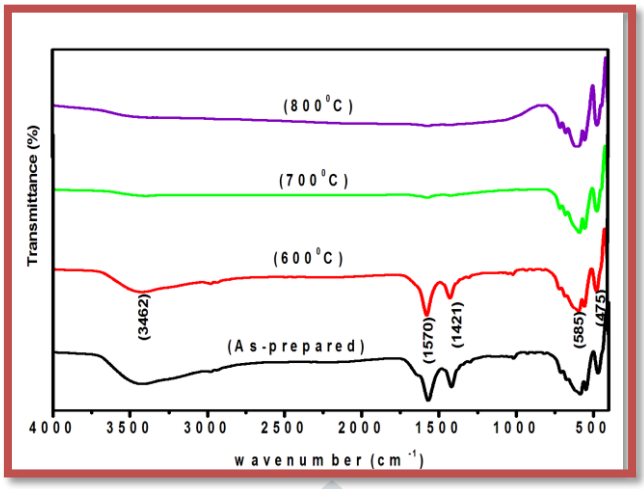


**Fig. 4 FT-IR analysis of $Li_{0.5}Fe_{2.5}O_4$ nanoparticles.**

The $\upsilon_1$ bands appear at 585 $cm^{-1}$ is related to the metal-oxygen vibrations in the tetrahedral site together with an additional band close to 3462 $cm^{-1}$. The appearance of the supplementary band with another peak attributed to the presence of two different covalent ions in the tetrahedral sites could be only assigned to $Fe^{3+}$ -$O^{2-}$ [13]. When the various heat treatments such as 600 °C, 700 °C and 800 °C, which is clearly shown with strength in the $Li_{0.5}Fe_{2.5}O_4$ structure. However, all the synthesized sample calcinations temperature increases while the hydroxyl groups have completely disappeared and the formation lower frequency.

## 3.4 FE-SEM with EDAX

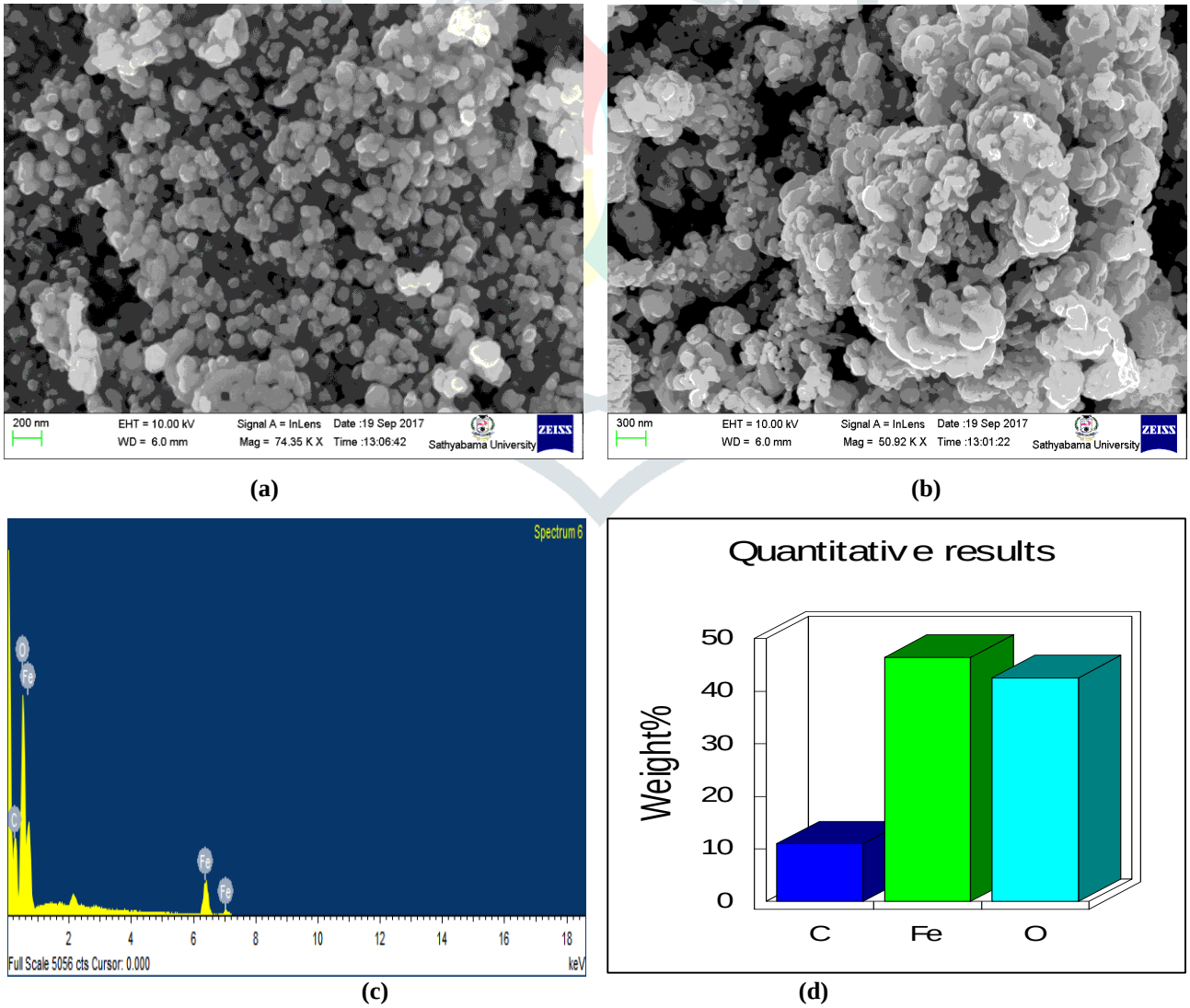


**Fig.5 FE-SEM of the $Li_{0.5}Fe_{2.5}O_4$ nanoparticles calcined at 700 °C (a) 200nm magnification , (b) 300nm magnification**

**(c) EDAX spectrum and (d) Corresponding atomic weight percentage**

Fig.5 (a), (b) indicate that the FE-SEM images of $Li_{0.5}Fe_{2.5}O_4$ nanoparticles calcined at 700 °C with the different magnifications. The micrographs image showed that the clear morphology with homogeneously and well crystallinity of $Li_{0.5}Fe_{2.5}O_4$ nanoparticles and it was spherical in nature with individual particles and agglomerated at some places. Related results were observed by Shon et al., [14]. Fig.5 (c) EDAX is used for the quantitative chemical analysis of the materials are composed Fe, O. In the EDAX spectrum could not show the Li due to the fact of EDAX detector cannot detect elements with atomic number less than four, hence Li metal cannot be detected by this technique [15]. Fig 5 (d) corresponding atomic weight percentages of EDAX spectrum.

## 3.5 Magnetic studies

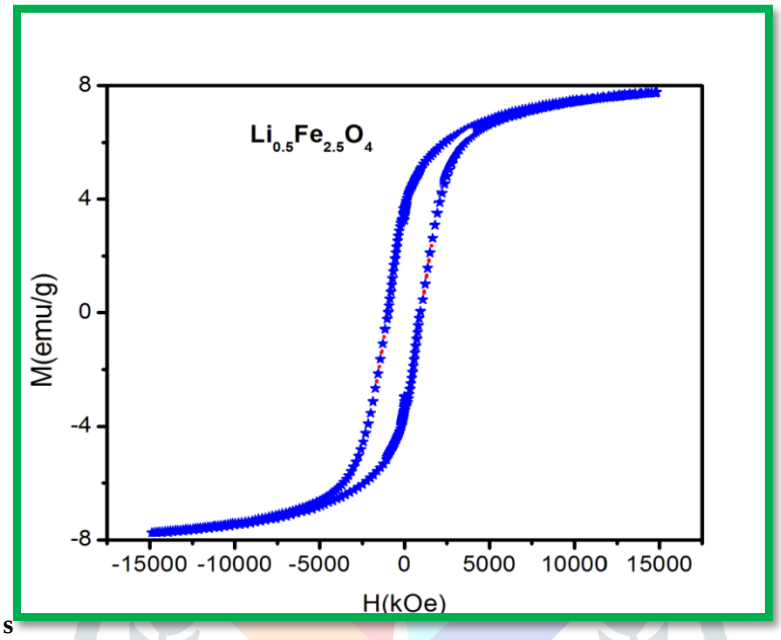


s

**Fig.6 Hysteresis loop of $Li_{0.5}Fe_{2.5}O_4$ nanoparticles**

Fig.6, illustrates the vibrating sample magnetometer measurements for lithium ferrite nanoparticles recorded at room temperature for applied field in the range of -15000 to +15000 generally lithium ferrite nanoparticles have inverse spinel structure, where $Li^{+1}$ have (tetra) $Fe^{3+}$ (octa) which is A and B sites. In the present study showed that the saturation magnetization (Ms) coercivity (Hc) and retentivity (Mr) values are calculated. The prepared materials were ferromagnetic nature and measured for magnetization values Such as saturation magnetization (Ms) 0.83074 emu/g, coercive field (Hc) 86.918 Oe and magnetic retentivity (Mr) 0.0100753emu/g remittances. In moreover the saturation magnetization (Ms) value is higher in the present work and crystallite size 36nm. A similar value was reported by Dar et al., (16). Table 2 showed the prepared materials were ferromagnetic nature and measured for magnetization values also tabulated.

**Table 2. The magnetization values of lithium ferrite nanoparticles**

| Saturation magnetization (Ms) | Magnetic Coercivity (Hc) | Magnetic retentivity (Mr) |
|---|---|---|
| **0.83074 emu/g** | 86.918 Oe | 0.010075 emu/g |

## 3.6 Cyclic voltammeter

The CV graphs of $Li_{0.5}Fe_{2.5}O_4$ electrode material were recorded at various scan rates, such as 10 $mVs^{-1}$, 25 $mVs^{-1}$, 50 $mVs^{-1}$, 75 $mVs^{-1}$, and 100 $mVs^{-1}$. Fig.7 indicates that the cyclic voltammeter (CV) of $Li_{0.5}Fe_{2.5}O_4$ nanoparticles. The graph showed the shape of the curves is ideal rectangular for an oxidation state and a reductive state which is the confirms of pseudo-capacitive nature of electrode material. The electrochemical properties $Li_{0.5}Fe_{2.5}O_4$ values can be calculated by the following relations

$$Cs = Q/ \Delta m * \Delta v.$$

Where,

Cs is the specific capacitance, Q the anodic and m is mass of the electrode material ($m_g$),

Δv is the scan rate ($mVs^{-1}$).

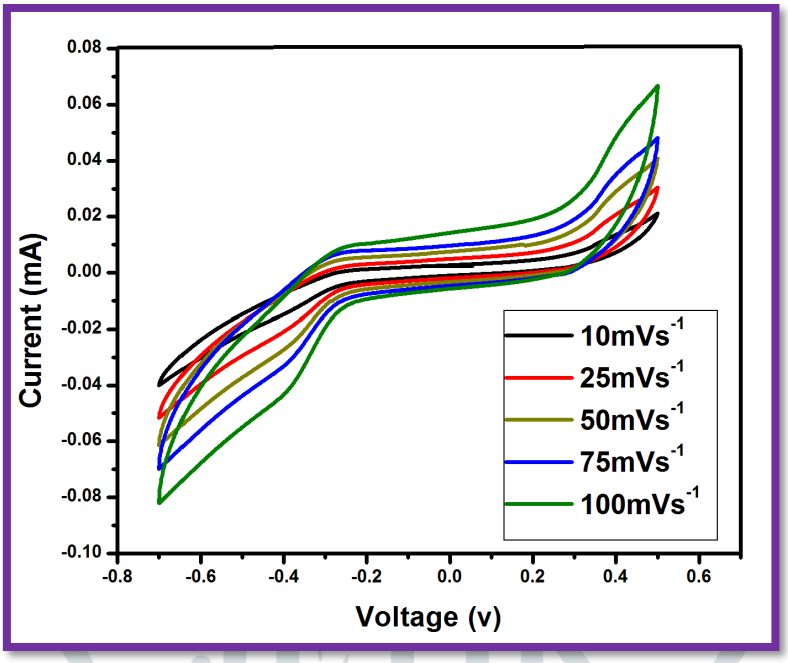


**Fig.7 Cyclic voltammeter (CV) of $Li_{0.5}Fe_{2.5}O_4$ nanoparticles**

The electrochemical property was performed in 0.2M tetra butyl ammonium for chlorate with a standard three-electrode setting and includes a group (working electrode), an Ag/AgCl (reference electrode) and a platinum cable (electrode of reference). In the current study showed higher specific capacitance is 569 $Fg^{-1}$ for the lower scan rate at 10 $mVs^{-1}$. For the reason low scan rate indicate that ion diffusion both inner and outer most of the penetration. Moreover, higher scan rate indicates that an ion diffusion occurs only for external surfaces, lower specific capacitance is 80 $Fg^{-1}$ for the higher scan rate at 100 $mVs^{-1}$ [17]. Prepared in $Li_{0.5}Fe_{2.5}O_4$ electrode material wear and excellent crystallinity with the suitable potential growing material. Table 3 showed the different scan rate, with specific capacitances from cyclic voltammeter also tabulated.

**Table 3 Specific capacitance values with different scan rates**

| Scan rates ($mVs^{-1}$) | 10 | 25 | 50 | 75 | 100 |
|---|---|---|---|---|---|
| Specific capacitances ($Fg^{-1}$) | 569 | 421 | 228 | 92 | 80 |

## 4. Conclusion

In summary, TG/DTA study confirms that the Exothermic and endothermic behavior of as-prepared samples. TG curves helps thermal stability of prepared sample and optimized calcination. No weight loss was predicted beyond 561 °C due to the stable phase of $Li_{0.5}Fe_{2.5}O_4$ nanoparticles. XRD study revealed that well crystalline nature with average crystallite size, lattice parameter was estimated. Surface morphology suggests that cubic symmetric with a spherical shape. EDAX feature revealed that the presence of elements such as Fe, O and $Li^{1+}$ (Monovalent). Lithium Iron peak is absent due to fact of lower density of the materials. FTIR study confirmed that the absorption band around at 600-400 $cm^{-1}$ corresponds to the presence of metal oxygen stretching vibration of $Li_{0.5}Fe_{2.5}O_4$ nanoparticles. Magnetization studies confirmed ferromagnetic nature and measured for magnetization values such as saturation (Ms) 0.83074 emu/g, coercive field (Hc) 86.918Oe and retentivity (Mr) 0.010075emu/g. Impedance spectroscopy confirmed that the amount of charge transfer resistance and clear semicircle drawn. However, these materials for electrochemical capacitor. From the CV study the higher capacitance value 569 $Fg^{-1}$ was observed in the lower scan rate of 10 $mVs^{-1}$. Hence it is suitable for electrochemical performances.

## References

1. Cheruku, R., Govindaraj, G. and Vijayan, L., 2017. Electrical relaxation, optical and magnetic studies of nanocrystalline lithium ferrite synthesized by different chemical routes. Materials Research Express, 4(12), pp.1-14.
2. Mohanty, V., Cheruku, R., Vijayan, L. and Govindaraj, G., 2013. Synthesis, structure and electrical conductivity studies of inverse spinel $Li_{0.5}Fe_{2.5}O_4$ Ind. J. of Pure & Appl. Physics Vol. 51, may 2013, pp 381-384.

3. Dasari, M., Gajula, G.R., Rao, D.H., Chintabathini, A.K., Kurimella, S. and Somayajula, B., 2017. Lithium ferrite: The study on magnetic and complex permittivity characteristics. Processing and Application of Ceramics, 11(1), pp.7-12.
4. Arzhavitin, V.M., Efimova, N.N. and Ustimenkova, M.B., 2001. Anomalies of internal friction of ferrimagnetic spinel $Li_{0.5}Fe_{2.5}O_4$ in various structural states. Physics of the Solid State, 43(11), pp.2121-2125.
5. Hyun, S.W. and Kim, C.S., 2007. Crystallographic and Mössbauer studies ofz$Li_{0.5}Fe_{2.5}O_4$prepared by high temperature thermal decomposition and sol-gel methods. Journal of applied physics, 101(9), pp. 09M513-3.
6. Jović, N.G., Masadeh, A.S., Kremenovic, A.S., Antic, B.V., Blanusa, J.L., Cvjeticanin, N.D., Goya, G.F., Antisari, M.V. and Bozin, E.S., 2009. Effects of thermal annealing on structural and magnetic properties of lithium ferrite nanoparticles. The Journal of Physical Chemistry C, 113(48), pp.20559-20567.
7. Gatelytė, A., Jasaitis, D., Beganskienė, A. and Kareiva, A., 2011. Sol-gel synthesis and characterization of selected transition metal nano-ferrites. Materials Science, 17(3), pp.302-307.
8. Verma, V., Pandey, V., Singh, S., Aloysius, R.P., Annapoorni, S. and Kotanala, R.K., 2009. Comparative study of structural and magnetic properties of nano-crystalline $Li_{0.5}Fe_{2.5}O_4$ prepared by various methods. Physica B: Condensed Matter, 404(16), pp.2309-2314.
9. Abdulmajeed, I.M., AL-Shakarchi, E.K., Al-Dharob, M.H. and Elouadi, B., 2015, Preparation of Nanoparticle Li-Ferrite Materials by Different Chemical Method vol. 4 (2), 69-76.
10. Fu, L.J., Liu, H., Li, C., Wu, Y.P., Rahm, E., Holze, R. and Wu, H.Q., 2005. Electrode materials for lithium secondary batteries prepared by sol–gel methods. Progress in Materials Science, 50(7), pp.881-928.
11. Dey, S., Roy, A., Das, D. and Ghose, J., 2004. Preparation and characterization of nanocrystalline disordered lithium ferrite by citrate precursor method. Journalof magnetism and magnetic materials, 270(1-2), pp.224-229.
12. Touthang, J., Maisnam, M., Singh, W.S. and Phanjoubam, S., 2016. Preparation of lithium ferrite nanoparticles by high energy ball milling and characterizations. International Journal of Engineering Research and Applications, 6(11), pp.08-11.
13. Singhal, S., Namgyal, T., Jauhar, S., Lakshmi, N. and Bansal, S., 2013. $LiFe_5O_8$ prepared by sol–gel synthesis: microstructural and morphological effects by organic and inorganic templates. Journal of sol-gel science and technology, 66(1), pp.155-162.
14. Sohn, R.S.T.M., Macedo, A.A.M., Costa, M.M., Mazzetto, S.E. and Sombra, A.S.B., 2010. Studies of the structural and electrical properties of lithium ferrite ($LiFe_5O_8$). Physica Scripta, 82(5), pp.055702.
15. Cheruku, R., Vijayan, L. and Govindaraj, G., 2012. Electron Microscopic Studies on the Lithium Ion Conducting Materials Current microscopy Contributions to Advances in Science and technology 1312-1323.
16. Dar, M.A., Shah, J., Siddiqui, W.A. and Kotnala, R.K., 2012. Influence of Synthesis approach on structural and magnetic properties of lithium ferrite nanoparticles. Journal of Alloys and Compounds, 523, pp.36-42.
17. Zeng, H., Tao, T., Wu, Y., Qi, W., Kuang, C., Zhou, S. and Chen,Y., 2014. $Li_{0.5}Fe_{2.5}O_4$ nanoparticles as anodes for lithium ion batteries. RSC Advances, 4(44), pp. 23145-23148.